

BIOACTIVITY AND QUANTUM CHEMICAL CALCULATIONS OF A NEW COUMARINE DERIVATIVE AS A STRONG ANTIOXIDANT, ANTIMICROBIAL AND ANTI-CANCER SUBSTANCE

Pelin Koparir

Firat University, Vocational School, Department of Forensics Chemistry, 23169 Elazig, Turkey
mpelin23@hotmail.com

4-(((4-Ethyl-5-(thiophen-2-yl)-4H-1,2,4-triazol-3-yl)thio)methyl)-7-methyl-coumarin was synthesized, and its characterization was done with quantum chemical calculations and spectral techniques. The density functional method (B3LYP) with the 6-311G(d,p) basis set was used to calculate the molecular geometry, vibrational frequencies, and gauge, including atomic orbital (GIAO) ^1H and ^{13}C -NMR chemical shift values of the title compound in the ground state. The theoretical vibrational frequencies and chemical shift values agree well with the experimental results. DFT calculations of the density of states (DOS) and frontier molecular orbitals of the title compound were carried out at the B3LYP/6-311G(d,p) level of theory. In the present study, biological activities and molecular docking studies of this triazole ring containing coumarin derivative compound were carried out. Interactions with important residues in active sites were detected in molecular docking studies. In addition, in vitro analysis has shown that antimicroorganism activity is especially effective against bacterial organisms such as *E. coli*, *S. aureus*, *B. cereus*, and fungal organisms such as *C. albicans*, *C. tropicalis*. Also, the antioxidant capacity of the test compound was investigated by oxidative stress index (OSI) and radical scavenging power (DPPH.), and its antioxidant potential was found. In addition, it was determined by in vitro anticancer and SDS-PAGE analysis that the test compound does not cause a detrimental cytotoxic effect on healthy cell cultures such as HUVEC and has the potential for anticarcinogenic activity on MCF-7 and MKN-45 cancerous cell cultures.

Keywords: new coumarin; NMR; computational calculations docking; biological activity

БИОАКТИВНОСТ И КВАНТНО-ХЕМИСКИ ПРЕСМЕТКИ НА НОВ КУМАРИНСКИ ДЕРИВАТ КАКО СУПСТАНЦА СО СИЛНИ АНТИОКСИДАЦИСКИ, АНТИМИКРОБНИ И АНТИКАНЦЕРОЗНИ СВОЈСТВА

Беше синтетизиран 4-(((4-етил-5-(тиофен-2-ил)-4H-1,2,4-триазол-3-ил)тио)метил)-7-метил-кумарин, а неговата карактеризација е извршена со помош на квантно-хемиски пресметки и спектрални техники. Беше искористен методот на густина на функционалот (B3LYP) со 6-311G(d,p) како базен сет за да се пресметаат молекулската геометрија, вибрациските фреквенции и вредностите на поместувањата според методот на атомските орбитални инваријантни вредности (GIAO) за ^1H и ^{13}C -NMR на наведеното соединение во основна состојба. Теориските вибрациски фреквенции и вредностите на хемиските поместувања се во согласност со експерименталните резултати. DFT-пресметките на густината на состојбата (DOS) и на граничните молекулски орбитали на наведеното соединение беа извршени на B3LYP/6-311G(d,p) ниво на теорија. Во оваа студија беше одредена биолошката активност и беше извршена студија на молекулско припојување на триазолскиот прстен што го содржи кумаринскиот дериват. При студиите на молекулското припојување беа детектирани интеракции со важни резидуи на активните центри. Покрај тоа, анализата in vitro покажа дека антимикуробната активност е особено ефикасна против бактериските организми како што се *E. coli*, *S. aureus* и *B. cereus* и фунгицидни организми како *C. albicans* и *C. tropicalis*. Исто така, антиоксидацискиот капацитет на испитуваното соединение беше

испитан преку оксидациониот стрес-индекс (OSI) и моќта за чистење на радикали (DPPH), со што беше определен антиоксидациониот потенцијал. Дополнително, со помош на *in vitro* антиканцерната SDS-PAGE анализа, беше определено дека испитуваното соединение не предизвикува штетни цитотоксични ефекти на здравите клеточни култури како што се HUVEC и дека покажува антиканцерозен потенцијал врз канцерозни клеточни култури MCF-7 и MKN-45.

Клучни зборови: нов кумарин; NMR; компјутерски пресметки на припојување; биолошка активност

1. INTRODUCTION

Coumarin derivatives are compounds called benzopyrones, chemically containing a benzene ring and pyrone ring. They can be found naturally in the fruits, seeds, leaves, and roots of plants in high concentrations.¹⁻⁴ Coumarins have exhibited a wide variety of biological activities such as antimicrobial, antioxidant, and anti-cancer activity as they can form hydrogen bonds, hydrophobic bonds, electrostatic interactions, metal coordination, and Van der Waals interactions with proteins and enzymes. Therefore, they have found wide use in medicinal chemistry.⁵⁻⁸ In addition to being found naturally, coumarins can also be synthetically obtained using various synthesis methods.⁹⁻¹¹ The highly functional nature of these heterocyclic compounds causes these compounds to occupy an important place in drug design.¹²⁻¹⁶ Posaconazole, fluconazole, itraconazole, ketoconazole and voriconazole, etc. are azole antifungal agents that show good *in vitro* activity against variety of microorganisms.^{17,18} In contrast to these compounds with good antifungal activity, the nitrogen positions of the triazole ring that makes up our test compound are different. Also, we discuss how all of the groups that make up the chemical structure of the compound affect biological activity.

In this study, a 1,2,4-triazole containing coumarin compound 4-(((4-ethyl-5-(thiophen-2-yl)-4*H*-1,2,4-triazol-3-yl)thio)methyl)-7-methylcoumarin was synthesized by reaction of 4-ethyl-5-(thiophene-2-yl)-4*H*-1,2,4-triazole-3-thiol and 4-(chloromethyl)-7-methylcoumarin. Also, characterization of the title compound was confirmed by FT-IR, ¹H-NMR, and ¹³C-NMR. The chemical structure of the compound was determined, and the DFT calculations of this compound were made. In addition to investigating its antimicrobial, antioxidant, cytotoxic activities, molecular docking studies were also carried out. Here, our conformational study for the resulting compound was aimed at obtaining the most appropriate structural form, while at the same time being concerned with predicting the fundamental properties. The interactions of the test compound with the macromole-

cules of some microorganisms were revealed using the molecular docking approach.

2. EXPERIMENTAL SECTION

2.1. Chemical analyses

Infrared spectra were measured using a Perkin-Elmer FT-IR spectrophotometer. The ¹H and ¹³C NMR spectra were obtained using a Bruker AC-400 NMR spectrometer set to 400 MHz for ¹H and 100 MHz for ¹³C. Chemical shifts were referenced to tetramethylsilane after the compounds were dissolved in dimethyl sulfoxide (DMSO) (¹H- and ¹³C-NMR). Elemental analyses were done on a LECO-CHNS-938 and Aldrich or Merck supplied the chemicals.

Synthesis of 4-ethyl-5-(thiophene-2-yl)-4*H*-1,2,4-triazole-3-thiol (III). After 3 hours of refluxing thiophene-2-carbohydrazide (**I**) (0.01 mol), ethyl alcohol (50 ml), and ethyl isothiocyanate, solid thiosemicarbazide began to form in the reaction flask. After adding 0.15 mol of KOH to the solid, dissolution began. The reaction was stopped after 6 hours, and the pH was adjusted to 3–4 with HCl. The residue was poured onto crushed ice. The resulting solid was filtered, dried, and recrystallized from ethyl alcohol. FT-IR (KBr, cm⁻¹, ν): 3072–3107 (Ar-H), 2870–2960 (C-H), 1570 (C=N), 1263 (C=S), 715 (C-S-C); ¹H NMR (400 MHz, DMSO-d₆, δ, ppm): 1.23 (t, 3H, N-CH₂-CH₃, *J* = 7.2 Hz), 4.22 (q, 2H, -N-CH₂-CH₃, *J* = 7.2 Hz), 7.27 (dd, 1H, Ar-H, *J* = 4.0, 4.8 Hz), 7.68 (d, 1H, Ar-H, *J* = 3.2 Hz) 7.86 (d, 1H, Ar-H, *J* = 4.8 Hz), 13.98 (s, 1H, SH); ¹³C-NMR (100 MHz, DMSO-d₆, δ, ppm): 13.7, 39.7, 126.8, 128.9, 129.3, 130.3, 146.3, 167.5.

Synthesis of 4-(((4-ethyl-5-(thiophen-2-yl)-4*H*-1,2,4-triazol-3-yl)thio)methyl)-7-methylcoumarin. Potassium carbonate (K₂CO₃) (0.02 mol) was dissolved in 30 ml of dry acetone. This solution was treated with 4-(chloromethyl)-7-methylcoumarin (0.02 mol). Dropwise addition of 4-ethyl-5-(thiophene-2-yl)-4*H*-1,2,4-triazole-3-thiol (**III**) (0.02 mol) to this solution for 6 hours at room

temperature followed. The resulting solid was filtered, dried, and recrystallized from ethyl alcohol. Figure 1 depicts the synthesis and structure of the title compound. FT-IR (KBr, cm^{-1} , ν): 560-740 (S-C), 938 and 1266 (O-C), 1717 (C=O), 2937–3081 (Ar-H), 1474 (C=N); $^1\text{H-NMR}$ (400 MHz, DMSO- d_6 , δ , ppm): 1.17 (t, 3H, N- $\text{CH}_2\text{-CH}_3$, $J = 7.0$ Hz), 3.39 (s, 3H, Ar- CH_3 ,) 4.09 (q, 2H, N- $\text{CH}_2\text{-CH}_3$, $J = 6.9$ Hz), 4.62 (s, 2H, S- CH_2), 6.32 (s, 1H, H-C-

C=O), 7.27 (m, 3H, Ar-H + thiophene-H), 7.57 (s, 1H, Ar-H), 7.85 (m, 2H, Ar-H + thiophene-H); $^{13}\text{C-NMR}$ (100 MHz, DMSO- d_6 , δ , ppm): 15.3, 21.2 33.8, 40.2, 114.4, 115.6, 117.2, 125.4, 125.9, 128.0, 128.7, 129.6, 143.5, 149.4, 150.3, 151.4, 153.9, 160.1. Elemental analysis: $\text{C}_{19}\text{H}_{17}\text{N}_3\text{O}_2\text{S}_2$, Calculated: C, 59.51; H, 4.47; N, 10.96; S, 16.72. Found: C, 59.47; H, 4.49; N, 10.91; S, 16.55.

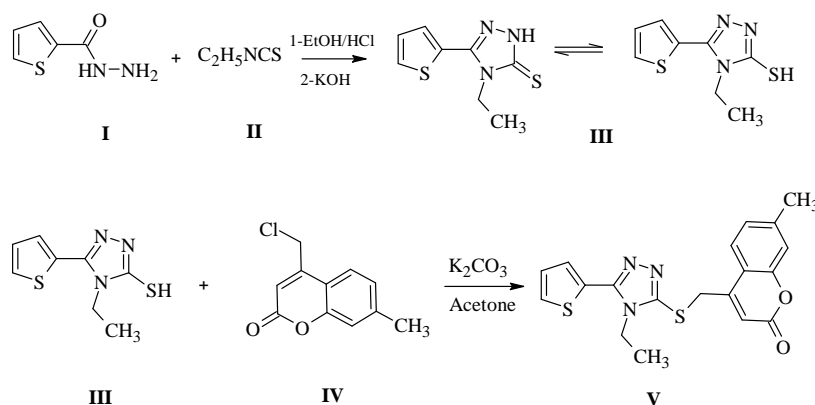


Fig. 1. Chemical structure for the title compound (V)

Computational methods. Gauss View5 and Gaussian 09 software were used to perform all theoretical calculations (optimization, IR, and NMR).^{19–21} B3LYP with a 6-311G(d,p) basis set was used to optimize the title compound^{22–26} _ENREF_20_ENREF_20_ENREF_20. Theoretical $^1\text{H-}$ and $^{13}\text{C-NMR}$ values were computed within the GIAO approach.²⁷ In nuclear magnetic resonance, calculations were used with DMSO as solvent. The harmonic vibrational frequencies for the optimized structure were assessed and the theoretically obtained frequency values are scaled by 0.958. The potential energy distribution (PED) of the title compound was calculated with VEDA 4 computer program. The density of state data (DOS) was calculated with Gausssum 3.0 software.²⁸

Molecular docking studies. The title compound was optimized-energy minimized using Gaussian 09 software at B3LYP/6-311G(d,p). The confirmation of the compound obtained here was recorded as PDB and was prepared for use in AutoDock 4.2²⁹ and AutoDock Vina software.³⁰ Heteroatoms or co-crystal ligand-centered grid box was defined in macromolecules in a regular space of 0.375 Å and with a size of 48×40×40 Å³, according to the size of the title compound. 1bqb and 6tz6 pdb files were obtained at the website of <http://www.rcsb.org/> and were modified using Maestro (Maestro, Schrödinger, LLC, New York,

NY, 2020.). The docking score was obtained by using the Lamarckian Genetic Algorithm for the AutoDock molecular docking program.

2.2. Biological activity

Antimicrobial assay. The effectiveness of the test compound against anti-microorganisms was determined by determining the minimum inhibitory concentration (MIC) against microorganisms by the "Microdilution Broth Method".³¹ Bacterial organisms, *S. aureus* (ATCC 29213), *P. aeruginosa* (ATCC 27853), *E. coli* (ATCC 25922), *B. cereus* (ATCC 11778), *K. pneumoniae* (ATCC 13883), *E. faecalis* (ATCC 29212), and fungal organisms, *C. albicans* (ATCC 10231) and *C. tropicalis* (DSM 11953), were used in our study. The test compound was dissolved in 40 % Dimethyl sulfoxide (DMSO) to make the stock solution. Mueller Hinton Broth (MHB, Accumix® AM1072) was used for bacteria, and Sabouraud Dextrose Broth (SDB, Himedia ME033) was used for fungi. Added 90 μl of MHB for antibacterial and SDB for antifungal with a sterile Pasteur pipette to the first wells of the microtiter plates. 50 μl of the medium was added to each of the other wells. Wells in row 11 were used as sterility control, and 100 μl of the medium was added to each.^{32,33} The 12th-place wells were used for re-

production control. 10 µl of the test compound from the stock solution was added to the first wells, while the others were diluted in series. A suspension with a turbidity of the McFarland 0.5 solution was prepared using microorganisms. A suspension of 50 µl of microorganisms was added to each well so that it was 5×10^5 CFU/ml for bacterial organisms and $0.5\text{--}2.5 \times 10^3$ CFU/ml for fungi. The plates were incubated at 37 °C for bacteria and 35 °C for fungal organisms for 16–24 hours. The MIC value was considered to be the first wells where the turbidity or appearance of

microorganisms decreased when evaluating the results. The test was repeated a total of 3 times.³⁴

Antioxidant-oxidant capacity. The total antioxidant capacity (TAC), total oxidant capacity (TOC), and oxidative stress index (OSI) of the test compound were calculated using Rel Assay Diagnostic commercial kits. While the Trolox standard was used for the TAC experiment, the hydrogen peroxide standard was used for the TOC experiment. The following formula was used to calculate the oxidative stress index (OSI) level.^{34,35}

$$OSI(AU) = \frac{TOC (\mu\text{mol H}_2\text{O}_2 \text{ equiv./l})}{TAC (\text{mmol Trolox equiv./l} \times 10)}$$

Cell culture studies. In the present study, the breast cancer cell culture (MCF-7) (human breast adenocarcinoma cell), human stomach cancer cell line (MKN-45; human gastric cancer cell line), and human endothelial cell line (HUVECs; human umbilical vein endothelial cell) were used. The cell lines are placed in vials of 25 cm² in the incubator (Corning-Sigma-Aldrich St. Louis, MO, USA). Each sample was cultured with Dulbecco's modified Eagle medium (DMEM) and 10 % Fetal Bovine Serum (FBS) at 37 °C with a CO₂ content of 5 %. When the density of the cells growth and morphology were monitored, when it reached the level of 90 %, the cultivation process was performed (Nueve MN 120). 200 µl of the mixture was placed in each of the 96 wells (5×10^3 cells in a 100 µl/plate space)³⁴ DMEM, FBS, and sterile phosphate buffer (PBS) were supplied commercially (Gibco Invitrogen).

MTT Test. In this study, the MTT analysis method was used to determine the effects of the test compound on cell cultures. For this, the test compound was used in various concentrations (1-10-100 mg/ml). Twenty-four hours after 10 µl of 12 mM MTT solution was added to the wells, it was incubated in a 5 % CO₂ oven at 37 °C for 4 hours. Then, 100 µl of SDS dissolved in 0.01 M HCl were added to dissolve the purple formazan crystals, and the solution was incubated in the oven. The absorbance of the purple color was measured at 570 nm with an Elisa reader, and the IC₅₀ results were calculated through GraphPad Prism 6.0 software (GraphPad Software, San Diego, CA, USA).³⁴

SDS-PAGE analysis. The effects of the test compound on cancer cell cultures were investigated by performing an SDS-PAGE analysis, thereby determining the effects of the test compound on certain protein secretions in cancerous and healthy cells.³⁶ Protein samples were analyzed by SDS-PAGE according to the explanations of Laemmli.³⁷

2.3. DPPH radical scavenging activity

The antiradical activity of the test compound was investigated according to the Blois method.³⁸ This method focuses on 1,1-diphenyl 2-picrylhydrazil radical (DPPH) elimination via free radical scavengers. DPPH is a free radical and has a red color. When this radical is scavenged by antioxidant compounds, the color changes from red to yellow. In our experiment, there was a decrease in absorption mixing at 517 nm. This indicates that the test compound caused an increase in antiradical activity in free radical scavenging (0.1 mM DPPH radical in the assay; butyl hydroxytoluene (BHT) (1 mg/ml) and the test compound were used as reference standards). The compound synthesized in the study and the standard compound were dissolved in ethyl alcohol at 1 mg/ml. The test compound and standard were used in the amounts of 50, 100, and 250 µg/ml, respectively. DMSO was added to form a total volume of 3 ml. After 30 min of incubation, absorbance measurements were made (UV-Vis Spectrophotometer: Shimadzu UV-1700 Spectrophotometer).

The calculation for DPPH radical scavenging activity was done according to the formulation presented below.

$$\% \text{ Radical scavenging power} = \left(Ac - \frac{As}{Ac} \right) \times 100$$

Ac: Absorbance of control, As: Absorbance of sample or standard

Statistical analysis. The SPSS 22.0 program³⁹ was used in the analysis of the data. All statistical analyses were performed at a 95 % confidence level using Student's *t*-test. For statistical correlation, $p \leq 0.05$ was defined as significant and $p \leq 0.01$ and 0.001 as highly significant.³⁹

3. RESULTS AND DISCUSSION

3.1. Molecular geometry

The optimized parameters of the title compound, such as bond lengths, bond angles, and dihedral angles, were obtained using the B3LYP/6-311G(d, p) method. The atomic numbering design of the theoretical geometric structure is given in Figure 2. The geometric parameters such as variation in bond lengths, bond angles, and dihedral angles are listed in Supplementary Table S1, due to substituents attached to the title compound. From the theoretical results, the aromatic ring was distorted from the regular hexagon due to the steric effect of the $-\text{CH}_3$ group. The C13-O1 and C12-O1 bond distances were determined as 1.362 Å and 1.367 Å, respectively, by using the B3LYP/6-311G(d,p) method. It has been reported that the actual bond length of C-O in the heterocyclic ring was 1.512 Å.^{40, 41} The result showed that the C13-O1 bond length was significantly reduced due to the fusion of the benzene ring with the α -pyrone ring through the O1 atom. The S1-C9 bond distance was observed at 1.837 Å whereas the S1-C1 bond distance was 1.764 Å. This may be due to the

substitution of C=N at the neighboring atom C1. Generally, the C-N bond was observed at 1.47 Å and the C=N bond length was observed at 1.33 Å, where the C-N values were higher than the C=N bond length.^{42,43} The C-N bond length of the triazole ring was computed at 1.372 Å, 1.385 Å for N3-C1, N3-C2, and for N3-C7 bound to ethyl, the molecule was observed at 1.465 Å. Further, the ethyl molecule C-N was higher than the triazole ring C-N. This may be due to the resonating structure of the triazole ring when compared with the ethyl molecule. The C1=N1 and C2=N1 bond lengths were determined as 1.310 Å and 1.315 Å, respectively, by using the B3LYP/6-311G(d,p) method. The DFT calculations give shortening of the angles at C13-C18-C17 by 2.610, C14-C15-C16 by 1.480, and enlargement in angles at C15-C16-C17 by 1.010, C14-C13-C18 by 1.560, and C16-C17-C18 by 1.060 from the normal angle 120° for benzene, which reveals that the substitution of CH_3 group at C15 position and the fusion of benzene ring with the α -pyrone ring at C13 and C18 position causes this distortion. For C2-C3-S2 and C4-C3-C2, they were calculated at 117° and 131° at the C3 position, respectively. The differences observed may be due to the presence of lone pair of electrons at the S2 position and active hydrogen at the C4 position. The orientation of the triazole ring of the title compound proved a notable discrepancy and was defined with torsion angle C2-N2-N1-C1 which was calculated at -0.048° for B3LYP/6-311G(d,p) level.

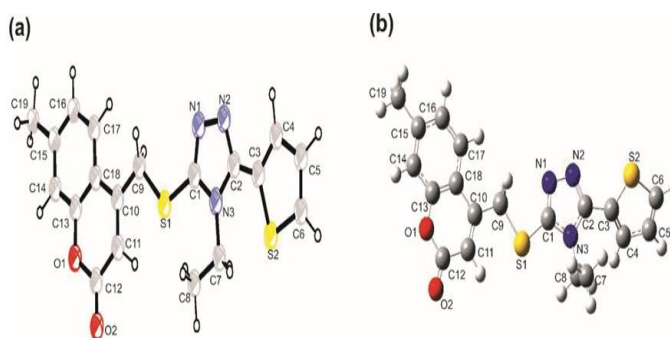


Fig. 2. The experimental geometric structure (a) and the theoretical geometric structure (b) of the title compound (with B3LYP/6-311G(d,p) level)

3.2. Nuclear magnetic resonance (NMR) spectra

Three stages of ^1H - and ^{13}C -NMR analysis were performed. When the ^1H - and ^{13}C -NMR spectra of the synthesized 4-ethyl-5-(thiophene-2-yl)-4*H*-1,2,4-triazole-3-thiol (**III**) were examined in

the first step of this work, the most characteristic peak was the SH/NH peak, which appears as a singlet at 13.98 ppm, as shown in Supplementary Figure S1. The title compound's experimental ^1H - and ^{13}C -NMR spectra were taken in DMSO in the second step of the work, and theoretical NMR calcula-

tions were performed using the B3LYP/6-311(d,p) basis set. There were some distinct peaks in the ^1H - and ^{13}C -NMR spectra of the title compound obtained in the study. The first and most distinctive peak is from the protons in the S-CH₂. Because of the electronegativity of the sulfur atom, hydrogen atoms close to it were set downfield. Experimental H shifts belonging to S-CH₂ were observed at 4.62 ppm as a singlet, the same H shifts were computed at 4.46 ppm and 4.42 ppm, respectively. The second of these is the ethyl fragment. The -CH₂ protons of the N-CH₂-CH₃ in the 4-position were observed to give a quartet peak at 4.09 ppm; the same protons were computed at 4.07 ppm and 4.21 ppm. While the -CH₃ protons showed triplet at 1.17 ppm, the same protons were calculated as at 1.64 ppm, 1.61 ppm, and 1.52 ppm, respectively. The carbons in the ^{13}C -NMR spectrum of the ethyl group were observed at 15.3 ppm for -CH₃ and at 33.8 ppm for -CH₂ as experimental, and the same carbons were computed at 16.6 ppm and 35.9 ppm, respectively. Carbon and hydrogen atoms close to the nitrogen atom are set downfield due to the electronegativity of the nitrogen atom. As a result, the electron charge density shifts away from these atoms and toward the nitrogen atom, and these atoms resonate downfield. The third of these is thiophene, the thiophene ring is a five-membered aromatic group. The unbound electron pair on the sulfur atom gives the ring six π electrons, and the structure becomes aromatic. However, these electrons, which are given to the ring, cause the hydrogens on the ring to resonate in the higher area. Due to the inductive effect of the sulfur atom, the hydrogen atom in the α position was observed in a lower area than the other two protons. While the hydrogen atom in the α position was shown at 7.85 ppm as experimental and as computed at 7.27 ppm, respectively, the other two protons were shown at 7.27 ppm as experimental and as computed at 7.45 ppm and 7.35 ppm, respectively. The fourth of these methyl protons is in the coumarin ring. While experimental H shifts belonging to the coumarin ring were observed at 3.39 ppm as a singlet, the same H shifts were computed at 3.11, 3.09 and 3.07 ppm, respectively. Besides the characteristic peaks, the disappearance of the SH/NH peak, which appears as a singlet at 13.98 ppm, was an important factor.

In the third step of the work, the interaction between the experimental and theoretical NMR data of the title compound was determined by a linear regression model. The equation was calculated as

$$\delta^1\text{H Exp} = -0.092 (\pm 0.173) + 0.990 (\pm 0.027) \delta\text{Calc.}$$

and the R2 value was calculated as 0.992. Besides, for the experimental and calculated ^{13}C -NMR values, the equation was

$$\delta^{13}\text{C Exp} = -0.089 (\pm 2.426) + 0.957 (\pm 0.019) \delta\text{Calc.}$$

and the R2 value was calculated as 0.994. The results are consistent with the literature.⁴⁴⁻⁴⁸ As can be seen from Supplementary Table S2 and Table S3, theoretical chemical shift outcomes of the title compound were compared with experimental data, showing generally closer values both for ^1H and ^{13}C -NMR. The chemical structure, ^1H , and ^{13}C -NMR spectra of the title compound are shown in Supplementary Figure S2 and Figure S3.

3.3. Fourier-transform infrared spectroscopy (FT-IR)

When the FT-IR spectra of the synthesized 4-ethyl-5-(thiophene-2-yl)-4H-1,2,4-triazole-3-thiol (**III**) were examined in the first step of this work, it was discovered that the C=O peak in the carboxylic acid hydrazides between 1635–1675 cm⁻¹ had vanished. In place of this peak, N=C=S peaks (amide bands) appeared at 1570, 1263, 1068, and 990 cm⁻¹. The most prominent peaks in the title compound obtained in the second step of the work were CO, CH, and CH₃ vibrations.

CO vibrations in the title compound were observed at two types of CO stretching vibrations: CO (C13-O1 and O1C12) stretching vibrations and C=O (C12=O2) stretching vibrations. C-O stretching vibrations were detected between 1250 and 850 cm⁻¹.⁴⁹ CO stretching vibrations values for the structural study of the title compound (O1-C12 and C13-O1) were observed experimentally at 938 and 1266 cm⁻¹ and calculated at 941 and 1270 cm⁻¹ for the B3LYP/6-311G(d,p) level. The C=O stretching frequency was observed in the range of 1650–1850 cm⁻¹. Due to its large change in dipole moment and its characteristic frequency, it is used to study a wide range of compounds.^{15,50} A very strong infrared absorption band at 1717 cm⁻¹ was easily assigned to the carbonyl vibration in the title compound and calculated as 1748 cm⁻¹ for B3LYP.

CH and CH₃ vibrations in the aromatic structures commonly show multiple bands between 3000 and 3100 cm⁻¹, which is the characteristic region for the C-H stretching vibrations.^{51,52} In the present study, the experimental C-H stretching vibration was observed in the FT-IR spectrum at 2937–3081 cm⁻¹. The same vibration was calculated theoretically in the range of 3144–2983 cm⁻¹

using the B3LYP method, and it showed a good correlation with the experimental data. The CH group usually gives rise to four fundamental bend vibrations: scissoring and rocking (in-plane bending), wagging, and twisting (out-of-plane bend). The C–H out-of-plane bending vibrations appeared in the region of 1000–675 cm^{-1} and C–H in-plane bending vibrations appeared in the region of 1400–1050 cm^{-1} .^{53,54} The C–H in-plane bending vibrations of the ring appeared at 1366–1086 cm^{-1} experimentally, and they were calculated theoretically in the range of 1383–1060 cm^{-1} for the B3LYP method. The C–H out-of-plane bending vibrations of the ring appeared at 1155–740 cm^{-1} experimentally, and they were calculated theoretically in the range of 1112–583 cm^{-1} for the B3LYP method. The CH_3 group usually gives rise to nine fundamental vibrations such as three bending modes, three stretching modes, two rocking modes, and a single torsional mode. The symmetric and asymmetric stretching vibrations of the methyl group normally appear at 2850–3000 cm^{-1} .⁵⁵

The calculated wave numbers of CH_3 group vibrations were observed at 2987 cm^{-1} (vs, coumarin), 2983 cm^{-1} (vs, triazole), 2917 cm^{-1} (vs, triazole), and 2906 cm^{-1} (vs, coumarin) for B3LYP method. The title compound contains some other important vibrations such as C=C, C-S, and C=N. The aromatic ring carbon-carbon (C=C) stretching modes appeared in the region of 1650–1200 cm^{-1} . In this work, the experimental C=C stretching vibrations were observed in the FT-IR spectrum at 1705–1217 cm^{-1} . The same vibrations were calculated theoretically in the range of 1714–1239 cm^{-1} using the B3LYP method. The C-S frequency values were shown in the region of 600–772 cm^{-1} in the literature.⁵⁶ These vibrations are observed in region 560–740 cm^{-1} experimentally and calculated theoretically in the range of 539–775 cm^{-1} for the B3LYP method. The C=N frequency values of the title compound appear at 1474 cm^{-1} and 1439 cm^{-1} . The calculated C=N frequency values have appeared at 1461 cm^{-1} and 1459 cm^{-1} . Also, the other levels of calculations can be seen in Supplementary Table S4. These results indicated some band shifts in the different substituent-triazole rings. Any discrepancy noted between the observed and the calculated frequencies may be due to the two facts: one is that the experimental results belong to the solid phase and theoretical calculations belong to the gaseous phase; the other is that the calculations have been done on a single molecule contrary to the experimental values recorded in the presence of intermolecular interactions.

3.4. Frontier molecular orbitals and global reactivity descriptors

Frontier molecular orbital theory is a molecular orbital theory application that describes HOMO-LUMO interactions. In the literature, global reactivity descriptors include global softness, global hardness, and electronegativity.^{57–61} The HOMO-1 electrons are delocalized in the coumarin ring, the HOMO electrons are delocalized in the triazole and thiophene rings, and the LUMO electrons are delocalized in the coumarin ring, while the LUMO+1 electrons are delocalized in the triazole and thiophene rings, as shown in Supplementary Figure S4. The energy separation between the HOMO and the LUMO is 4.0572 eV. This demonstrates that the energy gap reflects the molecule's chemical activity. These parameters for a molecule can be calculated using HOMO and LUMO energy values. Ionization potential is the minimum amount of energy required to remove an electron from a gaseous atom or molecule. The amount of energy released when an electron is added to a gaseous molecule is defined as electron affinity. Electronegativity is the tendency of an atom to attract electrons. Chemical hardness is a measure of how well molecules resist weight transfer. Higher chemical hardness molecules have little or no weight chemical softness.^{61,62} Supplementary Table S5 displays the electronic structure parameter values calculated by the B3LYP method with 6-311G(d,p). Because neighboring orbitals in the boundary region may have quasi-degenerate energy levels, considering only the HOMO and LUMO may not yield a realistic description of the frontier orbitals. As a result, the density of states (DOS) were calculated for both the gas phase and the solid phase using the Gauss Sum 3.0 software. The density of states diagram in the title compound is shown in Supplementary Figure S5.

3.5. Thermodynamic properties

The rotational temperatures, thermal energy, specific heat capacity, zero-point vibrational energy, rotational constants, and entropy of the title compound were calculated using the B3LYP/6-311G(d,p) main set at 298.150 K and 1.00 atm (Supplementary Table S6). The totality of thermodynamic data ensures useful knowledge for the investigation of thermodynamic energies and conjecture directions of chemical reactions using the second law of thermodynamics in thermo-chemical applications.

3.6. Biological activities

Anti-microorganism activity. The anti-microorganism activity of the test compound is given in Supplementary Table S7. It has been reported to be meaningful when the MIC is 0.1 mg/ml or less, mildly effective in the range of $0.1 < \text{MIC} \leq 0.625$ mg/ml, and weakly effective when greater than 0.625 mg/ml.⁶³ In the present study, it was found that the test compound was more effective on *Candida albicans*. Also, the test compound was found to have potent antimicrobial activity on *Escherichia coli*, *Staphylococcus aureus*, *Bacillus cereus*, and *Candida albicans*, *Candida tropicalis*. Also, it was determined to have a good effect on *P. aeruginosa*, *K. pneumoniae*, and *E. faecalis*. Overall, the test compound has a discernible antimicrobial activity on the eight microorganisms studied.

Antioxidant effect. The antioxidant potential of a compound is often due to its ability to reduce or transform the effects of oxidants. The therapeutic activities of the compounds can be thought to be due to their good antioxidant capacity.^{64,65} It is important to evaluate the oxidant and antioxidant capacities of the compounds depending on their chemical structures separately in terms of calculating the oxidative stress index.³⁴ The antioxidant capacity of the title compound, the oxidant capacity, and the oxidative stress index, as the ratio of these two capacities, are given in Supplementary Table S8. According to the results of the experiments, the oxidant value of the synthesized compound was 6.999 ± 0.518 , while its antioxidant value was 19.896 ± 0.712 . As a result, it is seen that the oxidative stress index was 0.037 ± 0.654 . It can be stated that the test compound is a good source of antioxidants together with its higher antioxidant capacity and lower oxidative stress index.

Cytotoxicity effect. The test compound was applied to 3 different cell lines (MCF-7, HUVEC, and MKN-45) at varying concentrations (1, 10, 100 $\mu\text{g/ml}$). The IC₅₀ values obtained after 24-hour incubation are given in Supplementary Table S9. If the IC₅₀ values are usually well above 10 μM , it can be assumed that the compound does not have a significant cytotoxic effect on these cell lines (Supplementary Figure S6). Accordingly, when the cytotoxic activity of the test compound on the HUVEC (normal human cell line) cell line is examined, it is seen that it does not have a harmful cytotoxic effect on healthy cells. Also, the test compound showed pronounced cytotoxicity against all of the tested cancer cell lines. In chemotherapy, it is very important to use agents that only kill cancerous cells and do not harm other healthy cells.

The results indicated that the test compound did not show any toxicity for healthy cells and the test compound selectively inhibited the growth of cancer cells (especially MCF-7) only.

SDS-PAGE analysis. According to the protein bands we obtained in the results of the study, significant differences were found in protein expression with a molecular weight of 66.2 kDa. According to the gel images in (Supplementary Figures S7 and S8), it was determined that the protein expression levels in row 4 were higher than the control group in rows 2 and 3.

Albumin protein is in the nonenzymatic antioxidant protein group represented by a molecular weight of 66.2 kDa. It is known to bind the HOCl radical and some protein and metal ions, and the albumin levels in cancer cases remain low compared to the control group. However, it is known that in some cases, the structure of albumin can be modified compared to normal albumin. Therefore, more research is needed on this subject. On the other hand, it was determined that the test compound increased the levels of less expressed protein in cancer cells. This result reveals the necessity of further studies with molecular techniques.

Antiradical scavenging activity. The reducing power of DPPH radicals was obtained by calculating the percent inhibition values after they were detected by absorbance reduction at 517 nm induced by the test compound. The calculated results are given in Supplementary Table S10. The results revealed that the test compound showed a decent level of activity, close to the standard antioxidant BHT (Supplementary Figure S9). DPPH is a stable, free radical and accepts an electron or hydrogen radical to become a stable diamagnetic molecule. Therefore, it was concluded that there is a large scope for further study in order to more clearly reveal the structure-activity relationship.

Molecular docking. According to the crystallographic structures of “*aureolysin*, *Staphylococcus aureus metalloproteinase*” and “*Candida albicans Calcineurin A*, *Calcineurin B*, FKBP12 and FK506 (*Tacrolimus*)”, the main binding site has been determined to be around heteroatoms or a small molecule. It has been declared that FK506 (*Fujimycin*) for 6TZ6, Zn²⁺, and Ca²⁺ atoms for 1BQB macromolecules interact with active sites as binding sites.^{66,67} Calcium ions have been reported to bind to residues found in Asp140, 176–187, and 190–197 cycles. It has been previously reported that zinc ion binds to residues such as His144, His148, and Glu168.⁶⁶ For FK506, it has been reported to bind to residues found in the 6TZ6 active site. The hydrogen bond of our test compound with

residue A:TRP401 was the same as FK506 (<https://www.rcsb.org/3d-view/ngl/6tz6>). The test compound binding mode was similar to Fujimycin in 6TZ6 (Fig. 3). Residues participating Pi Cation, Pi-Pi Stacking, and H-bonds with the title compound are shown in Table S11. Similar interactions were observed on all macromolecules with molecular docking studies for the title compound (Supplementary Table S11). 2D interaction modes (Fig. 4) and 3D interaction modes (Fig. 5) for test compounds with macromolecule active sites were determined. Ligand binding types and residues of macromolecules were visualized by Maestro software.⁶⁸ When the results of the molecular docking studies were compared with the results of the biological activity studies, it can be determined that the results were parallel. According to the results of both molecular docking and antimicrobial activity studies, it can be stated that the effect of the test compound on *Candida albicans* is stronger than on other microorganisms.

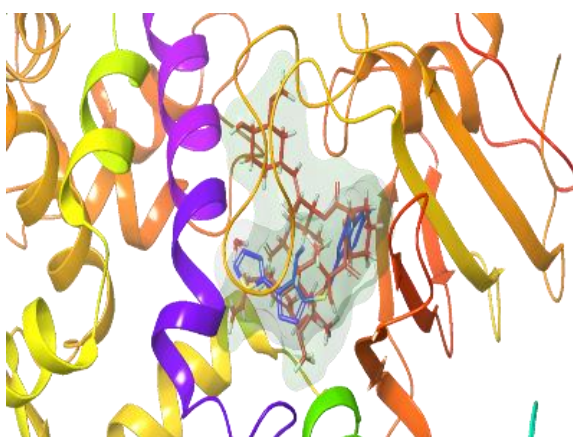


Fig. 3. The title compound (blue) and C:FK506 (red) are presented in the 6TZ6 binding cavity (molecular surface rendered in light green)

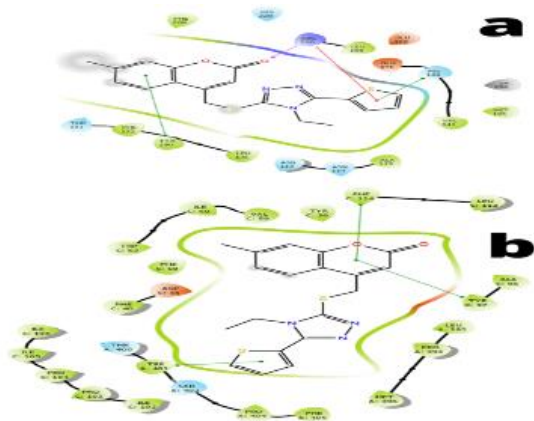


Fig. 4. 2D interactions diagram for title compound at active sites of 1BQB (a) and 6TZ6 (b)

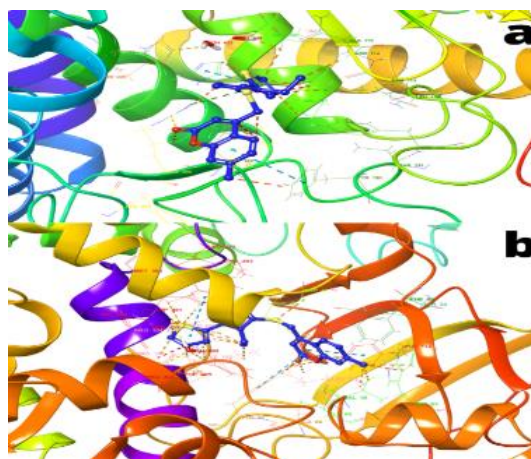


Fig. 5. 3D interactions for title compound at active sites of 1BQB (a) and 6TZ6 (b)

4. CONCLUSIONS

The title compound containing a 1,2,4-triazole coumarin derivative was synthesized, and characterization was confirmed by FT-IR, ¹H-, and ¹³C-NMR. Spectroscopic and electronic properties of the title compound were examined both experimentally (in vitro) and theoretically (in silico), and biological activity studies were carried out. The optimized geometric parameters (bond, lengths, and bond angles) were theoretically determined at the B3LYP/6-311G(d,p) level of the title compound. The chemical shifts were compared with experimental data in DMSO solution, showing a very good agreement both for ¹H and ¹³C-NMR chemical shifts. An agreement was determined between the theoretical and experimental results with regard to the accurate allocation of the vibrational frequencies to the molecular structure based on the theoretical calculations. Thermodynamic features and HOMO and LUMO energies in the ground state of the title compound were calculated by using the density function. It turned out that the test compound had a high antioxidant capacity but also contained a moderate level of oxidant. It was observed that the oxidative stress index (OSI), which is important in evaluating the antioxidant/oxidant ratio of the test compound, was very low. It was also determined that its antiradical activity was good. According to all these results, it can be said that the test compound has good antioxidant potential with its high antioxidant capacity and lower oxidative stress index and antiradical properties. The results indicated that the test compound could productively inhibit the growth of tested microbial organisms, and it displayed an extensive antimicrobial spectrum. Also, the test compound did not show any toxicity, suggesting our test compound

selectively inhibited the growth of cancer cells only. The therapeutically beneficial effects of synthetic compounds are often associated with their antioxidant properties. Therefore, they are suitable for use in the cosmetic, food, and pharmacological industries to reduce oxidative damage. In this respect, we think that our study results and the test compound will contribute to the literature.

Acknowledgment. The authors would like to acknowledge the help of Prof. Dr. Metin Koparir, Chemistry Department, Firat University in Turkey, in carrying out this work.

REFERENCES

- Borges, F.; Roleira, F.; Milhazes, N.; Santana, L., Uriarte. Simple coumarins and analogues in medicinal chemistry: occurrence, synthesis and biological activity. *Curr. Med. Chem.* **2005**, *12*, 887–916. DOI: 10.2174/0929867053507315
- Borges Bubols, G.; Rocha Vianna, D.; Medina-Reimon, A.; Von Poser, G.; Maria Lamuela-Raventos, R.; Lucia Eiffler-Lima, V.; Cristina Garcia, S., The antioxidant activity of coumarins and flavonoids. *Mini Rev. Med. Chem.* **2013**, *13*, 318–334. DOI: 10.2174/138955713804999775
- Davis, R. A.; Vullo, D.; Maresca, A.; Supuran, C. T.; Poulsen, S. A., Natural product coumarins that inhibit human carbonic anhydrases. *Bioorg. Med. Chem.* **2013**, *21*, 1539–1543. DOI: 10.1016/j.bmc.2012.07.021
- Zhang, L.; Jiang, G.; Yao, F.; He, Y.; Liang, G.; Zhang, Y.; Hu, B.; Wu, Y.; Li, Y.; Liu, H., Growth inhibition and apoptosis induced by osthole, a natural coumarin, in hepatocellular carcinoma. *PLoS one.* **2012**, *7*, e37865. DOI: 10.1371/journal.pone.0037865
- Peng, X. M.; Damu, G. L. V.; Zhou, H., Current developments of coumarin compounds in medicinal chemistry. *Curr. Pharm. Des.* **2013**, *19*, 3884–3930. DOI: 10.2174/1381612811319210013
- Thakur, A.; Singla, R.; Jaitak, V., Coumarins as anticancer agents: a review on synthetic strategies, mechanism of action and SAR studies. *Eur. J. Med. Chem.* **2015**, *101*, 476–495. DOI: 10.1002/CHIN.201541254
- Karataş, M. O.; Uslu, H.; Sarı, S.; Alagöz, M. A.; Karakurt, A.; Alici, B.; Bilen, C.; Yavuz, E.; Gencer, N.; Arslan, O., Coumarin or benzoxazinone based novel carbonic anhydrase inhibitors: Synthesis, molecular docking and anticonvulsant studies. *J. Enzyme. Inhib. Med. Chem.* **2016**, *31*, 760–772. DOI: 10.3109/14756366.2015.1063624
- Karataş, M. O.; Uslu, H.; Alici, B.; Gökçe, B.; Gencer, N.; Arslan, O., Some coumarins and benzoxazinones as potent paraoxonase 1 inhibitors. *J. Enzyme. Inhib. Med. Chem.* **2016**, *31*, 1386–1391. DOI: 10.3109/14756366.2015.1063624
- Potdar, M. K.; Mohile, S. S.; Salunkhe, M. M., Coumarin syntheses via pechmann condensation in Lewis acidic chloroaluminate ionic liquid. *Tetrahedron Lett.* **2001**, *42*, 9285–9287. DOI: 10.1002/CHIN.200212169
- Perkin, W., XXIII On the hydride of aceto-salicyl. *J. Chem. Soc.* **1868**, *21*, 181–186. DOI:10.1039/js8682100181
- Knoevenagel, E., Condensation of malonic acid with aromatic aldehydes with ammonia and amines. *J. Am. Chem. Soc.* **1898**, *31*, 2596–2619. DOI: org/10.1002/cber.18980310308
- Karataş, M. O.; Uslu, H.; Alici, B.; Gökçe, B.; Gencer, N.; Arslan, O.; Arslan, N. B.; Özdemir, N., Functionalized imidazolium and benzimidazolium salts as paraoxonase 1 inhibitors: synthesis, characterization and molecular docking studies. *Bioorg. Med. Chem.* **2016**, *24*, 1392–1401. DOI: 10.1016/j.bmc.2016.02.012
- Bayazeed, A.; Alshehrei, F.; Muhammad, Z. A.; Al-Fahemi, J.; El-Metwaly, N.; Farghaly, T. A., Synthesis of coumarin-analogues: analytical, spectral, conformational, MOE-docking and antimicrobial studies. *Chemistry Select.* **2020**, *5*, 1–1. DOI: 10.1002/slct.201904724
- Koparir, P., Synthesis, antioxidant and antitumor activities of some of new cyclobutane containing triazoles derivatives. *Phosphorus. Sulfur. Silicon. Relat. Elem.* **2019**, *194*, 1028–1034. DOI: 10.1080/10426507.2019.1597363
- Koparir, P.; Karaarslan, M.; Orek, C.; Koparir, M., Synthesis and in-vitro antimicrobial activity of novel aminophosphinic acids containing cyclobutane and 1,3-thiazole. *Phosphorus. Sulfur. Silicon. Relat. Elem.* **2011**, *186*, 2368–2376. DOI: 10.1080/10426507.2011.604660
- Parlak, A. E.; Tekin, S.; Karatepe, A.; Koparir, P.; Telceken, H.; CeribasıA. O.; Karatepe, M., In vitro and histological investigation of antitumor effect of some triazole compounds in colon cancer cell line. *J. Cell. Biochem.* **2019**, *120*, 11809–11819. DOI:org/10.1002/jcb.28460
- Blanco, M. T.; Cañadas, J.; García-Martos, P.; Marín, P.; García-Tapia, A.; Rodríguez, J., In vitro activities of posaconazole, fluconazole, itraconazole, ketoconazole and voriconazole against *Candida glabrata*. *Rev. Esp. Quimioter.* **2009**, *22*, 139–143.
- Saravolatz, L. D.; Johnson, L. B.; Kauffman, C. A., Voriconazole: a new triazole antifungal agent. *Clinical Infectious Diseases.* **2003**, *36*, 630–637. DOI: 10.1086/367933
- Raj, R.; Gunasekaran, S.; Gnanasambandan, T.; Seshadri, S., Combined spectroscopic and DFT studies on 6-bromo-4-chloro-3-formyl coumarin. *Spectrochim. Acta A Mol. Biomol. Spectrosc.* **2015**, *139*, 505–514. DOI:org/10.1016/j.saa.2014.12.024
- Koparir, M.; Orek, C.; Koparir, P.; Sarac, K., Synthesis, experimental, theoretical characterization and biological activities of 4-ethyl-5-(2-hydroxyphenyl)-2H-1,2,4-triazole-3(4H)-thione. *Spectrochim. Acta A Mol. Biomol. Spectrosc.* **2013**, *105*, 522–531. DOI: org/10.1016/j.saa.2012.12.052
- Cansiz, A.; Orek, C.; Koparir, M.; Koparir, P.; Cetin, A., 4-allyl-5-pyridin-4-yl-2, 4-dihydro-3H-1, 2, 4-triazole-3-

- thione: synthesis, experimental and theoretical characterization. *Spectrochim. Acta A Mol. Biomol. Spectrosc.* **2012**, *91*, 136–145.
DOI: org/10.1016/j.saa.2012.01.027
- (22) Kalaiarasi, N.; Manivarman, S., Synthesis, spectroscopic characterization, computational exploration of 6-(2-(2, 4-dinitrophenylhydrazano)-tetrahydro-2-thioxopyrimidin-4 (1h)-one. *Orient. J. Chem.* **2017**, *33*, 304–317.
DOI: 10.13005/ojc/330136
- (23) Inkaya, E.; Dinçer, M.; Çukurovalı, A.; Yılmaz, E., 2-chloro-N-[4-(3-methyl-3-phenylcyclobutyl)-1, 3-thiazol-2-yl]-N'-(naphthalen-1-ylmethylidene) acetohydrazide. *Acta Crystallographica Section E: Structure reports online.* **2011**, *67*, o310-o310.
DOI: org/10.1107/S1600536811000183
- (24) Dinçer, M.; Özdemir, N.; Yılmaz, İ.; Çukurovalı, A.; Büyükgüngör, O., 1-methyl-1-phenyl-3-[1-hydroxyimino-2-(succinimido) ethyl] cyclobutane. *Acta Crystallogr. C Struc. Chem.* **2004**, *60*, o674-o676.
DOI: 10.1007/S11224-008-9387-7
- (25) İnkaya, E.; Dinçer, M.; Ekici, Ö.; Cukurovalı, A., 1-(3-methyl-3-mesityl)-cyclobutyl-2-(5-pyridin-4-yl-2H-[1,2,4] triazol-3-ylsulfanyl)-ethanone: X-ray structure, spectroscopic characterization and DFT studies. *Spectrochim. Acta A Mol. Biomol. Spectrosc.* **2013**, *101*, 218–227.
DOI: 10.1016/j.saa.2012.09.091
- (26) Jameson, C. J.; Dios, A. C., Ab initio calculations of the intermolecular chemical shift in nuclear magnetic resonance in the gas phase and for adsorbed species. *J. Chem. Phys.* **1992**, *97*, 417–434.
DOI: 10.1063/1.463586
- (27) Orek, C.; Koparir, P.; Koparir, M., N-cyclohexyl-2-(5-(4-pyridyl)-4-(p-tolyl)-4H-1,2,4-triazol-3-ylsulfanyl) -acetamide dihydrate: synthesis, experimental, theoretical characterization and biological activities. *Spectrochim. Acta A Mol. Biomol. Spectrosc.* **2012**, *97*, 923–934.
DOI: org/10.1016/j.saa.2012.07.082
- (28) Lin-Vien, D.; Colthup, N. B.; Fateley, W. G., Grasselli, J. G., The Handbook of Infrared and Raman Characteristic Frequencies of Organic Molecules. Elsevier, 1991.
- (29) Sarıkaya, E. K.; Dereli, Ö., Molecular structure and vibrational spectra of 7-methoxy-4-methylcoumarin by density functional method. *J. Mol. Struct.* **2013**, *1052*, 214–220. DOI: org/10.1016/j.molstruc.2013.08.024
- (30) Moghanian, H.; Mobinikhaledi, A.; Monjezi, R., Synthesis, spectroscopy (vibrational, NMR and UV–vis) studies, HOMO–LUMO and NBO analysis of 8-formyl-7-hydroxy-4-methylcoumarin by ab initio calculations. *J. Mol. Struct.* **2013**, *1052*, 135–145.
DOI: org/10.1016/j.molstruc.2013.08.043
- (31) Cansiz, A.; Cetin, A.; Kutulay P.; Koparir, M., Synthesis of tautomeric forms of 5-(2-hydroxyphenyl)-4-substituted-3H-1, 2, 4-triazole-3-thione. *Asian J. Chem.* **2009**, *21*, 617.
- (32) Smith, B. C., *Infrared Spectral Interpretation: A Systematic Approach*, CRC Press, 1998.
- (33) Tammer, M.; Sokrates G., *Infrared and Raman Characteristic Group Frequencies: Tables and Charts*, Springer, 2004.
- (34) Sarıkaya, E. K.; Dereli, Ö.; Erdoğan, Y.; Güllüoğlu, M., Molecular structure and vibrational spectra of 7-ethoxycoumarin by density functional method. *J. Mol. Struct.* **2013**, *1049*, 220–226.
DOI: org/10.1016/j.molstruc.2013.06.026
- (35) Sajan, D.; Erdogdu, Y.; Reshmy, R.; Dereli, O.; Thomas K. K.; Joe, I. H., DFT-based molecular modeling, nbo analysis and vibrational spectroscopic study of 3-(bromoacetyl) coumarin. *Spectrochim. Acta A Mol. Biomol. Spectrosc.* **2011**, *82*, 118–125.
DOI: 10.1016/j.saa.2011.07.013
- (36) Chattaraj, P. K.; Giri, S., Stability, reactivity, and aromaticity of compounds of a multivalent superatom. *J. Phys. Chem. A.* **2007**, *111*, 11116–11121.
DOI: 10.1021/jp0760758
- (37) Geerlings, P.; De Proft, F.; Langenaeker, W., Conceptual density functional theory. *Chem. Rev.* **2003**, *103*, 1793–1874. DOI: 10.1021/cr990029p
- (38) Parr, R. G.; Pearson, R. G., Absolute hardness: companion parameter to absolute electronegativity. *J. Am. Chem. Soc.* **1983**, *105*, 7512–7516.
DOI: org/10.1021/ja00364a005
- (39) Parr, R. G.; Szentpaly, L. V.; Liu, S., Electrophilicity index. *J. Am. Chem. Soc.* **1999**, *121*, 1922–1924.
DOI: org/10.1021/ja00364a005
- (40) Pearson, R. G. Absolute Electronegativity and Hardness: Applications to Organic Chemistry. *J. Org. Chem.* **1989**, *54*, 1423–1430. DOI: org/10.1021/jo00267a034
- (41) Pearson, R. G., Absolute electronegativity and hardness correlated with molecular orbital theory. *Proc. Natl. Acad. Sci. U. S. A.* **1986**, *83*, 8440–8441.
DOI: 10.1073/pnas.83.22.8440
- (42) Awouafack, M. D.; McGaw, L. J.; Gottfried, S.; Mbouangouere, R.; Tane, P.; Spittler, M.; Eloff, J. N., Antimicrobial activity and cytotoxicity of the ethanol extract, fractions and eight compounds isolated from *Eriosema robustum* (Fabaceae). *BMC Complement Altern. Med.* **2013**, *13*, 289.
DOI: 10.1186/1472-6882-13-289
- (43) Di Guardo, A.; Sarac, M.; Gabardi, M.; Leonardis, D.; Solazzi, M.; Frisoli, A., Sensitivity analysis and identification of human parameters for an adaptive, underactuated hand exoskeleton. *International Symposium on Advances in Robot Kinematics*, Springer, 2018. DOI:10.1007/978-3-319-93188-3_51.
- (44) Koparir, P.; Parlak, A. E.; Karatepe, A.; Omar, R. A., Elucidation of potential anticancer, antioxidant and antimicrobial properties of some new triazole compounds bearing pyridine-4-yl moiety and cyclobutane ring. *Arab. J. Chem.* **2022**, 103957.
DOI: org/10.1016/j.arabjc.2022.103957
- (45) Banbula, A.; Potempa, J.; Travis, J.; Fernandez-Catalén, C.; Mann, K.; Huber, R.; Bode, W.; Medrano, F. J., Amino-acid sequence and three-dimensional structure of the Staphylococcus aureus metalloproteinase at 1.72 Å Resolut. *Struct.* **1998**, *6*, 1185–1193.
DOI:10.1016/S0969-2126(98)00118-X
- (46) Juvvadi, P. R.; Fox, D.; Bobay, B. G.; Hoy, M. J.; Gobeil, S. M. C.; Venters, R. A.; Chang, Z.; Lin, J. J.; Averette, A. F.; Cole, D. C.; Barrington, B. C.;

- Wheaton, J. D.; Ciofani, M.; Trzoss, M.; Li, X.; Lee, S. C.; Chen, Y.-L.; Mutz, M.; Spicer, L. D.; Schumacher, M. A.; Heitman, J.; Steinbach, W. J., Harnessing calcineurin-FK506-FKBP12 crystal structures from invasive fungal pathogens to develop antifungal agents. *Nat. Commun.* **2019**, *10*, 4275. DOI: org/10.1038/s41467-019-12199-1
- (47) Uddin, M.; Mustafa, F.; Rizvi, T. A.; Loney, T.; Suwaidi, H. A.; Al-Marzouqi, A. H. H.; Eldin, A. K.; Alsabeeha, N.; Adrian, T. E.; Stefanini, C., SARS-CoV-2/COVID-19: Viral genomics, epidemiology, vaccines, and therapeutic interventions. *Viruses.* **2020**, *12*, 526. DOI: org/10.3390/v12050526
- (48) Cansiz, A.; Orek, C.; Koparir, M.; Koparir, P.; Cetin, A., 4-allyl-5-pyridin-4-yl-2,4-dihydro-3H-1,2,4-triazole-3-thione: synthesis experimental and theoretical characterization. *Spectrochim. Acta A Mol. Biomol. Spectrosc.* **2012**, *91*, 136–145. DOI:10.1016/j.saa.2012.01.02
- (49) Dennington, R.; Keith, T. A.; Millam, J. M., *GaussView*. Shawnee Mission, KS., Semichem. Inc. **2009**.
- (50) Becke, A. D., Density-functional thermochemistry. III. The role of exact exchange. *J. Chem. Phys.* **1993**, *98*, 5648–5652. DOI:10.1063/1.464913
- (51) Omer, R. A.; Ahmed, L.; Koparir, M.; Koparir, P., Theoretical analysis of the reactivity of chloroquine and hydroxychloroquine. *Indian J. Chem.* **2020**, *59*, 1828–1834.
- (52) Ahmed, L.; Omer, R. A., Computational study on paracetamol drug. *J. Phys. Chem. Funct. Mater.* **2020**, *3*, 9–13.
- (53) Lee, C.; Yang, W.; Parr, R. G., Development of the Colle-Salvetti correlation-energy formula into a functional of the electron density. *Phys. Rev. B.* **1988**, *37*, 785–789. DOI:10.1103/PhysRevB.37.785
- (54) Wolinski, K.; Hinton, J. F.; Pulay, P., Efficient implementation of the gauge-independent atomic orbital method for NMR chemical shift calculations. *J. Am. Chem. Soc.* **1990**, *112*, 8251–8260. DOI:10.1021/JA00179A005
- (55) Rebaz, O.; Koparir, P.; Ahmed, L.; Koparir, M., Computational determination the reactivity of salbutamol and propranolol drugs. *Turk. Comput. Theor. Chem.* **2020**, *4*, 67–75. DOI:org/10.33435/tcandtc.768758
- (56) Sundaraganesan, N.; Ilakiamani, S.; Saleem, H.; Wojciechowski, P. M.; Michalska, D., FT-Raman and FT-IR spectra, vibrational assignments and density functional studies of 5-bromo-2-nitropyridine. *spectrochim. Acta A Mol. Biomol. Spectrosc.* **2005**, *61*, 2995–3001. DOI:10.1016/J.SAA.2004.11.016
- (57) Jamróz, M. H., Vibrational energy distribution analysis (VEDA): Scopes and limitations. *Spectrochim. Acta A Mol. Biomol. Spectrosc.* **2013**, *114*, 220–230. DOI: 10.1016/j.saa.2013.05.096
- (58) Morris, G. M.; Huey, R.; Lindstrom, W.; Sanner, M. F.; Belew, R. K.; Goodsell, D. S.; Olson, A. J., AutoDock4 and AutoDockTools4: Automated docking with selective receptor flexibility. *J. Comput. Chem.* **2009**, *30*, 2785–2791. DOI: 10.1002/jcc.21256
- (59) Trott, O.; Olson, A. J., AutoDock Vina: Improving the speed and accuracy of docking with a new scoring function, efficient optimization, and multithreading. *J. Comput. Chem.* **2010**, *31*, 455–461. DOI:10.1002/jcc.21334
- (60) Eloff, J. N., A Sensitive and quick microplate method to determine the minimal inhibitory concentration of plant extracts for bacteria. *Planta Med.* **1998**, *64*, 711–713. DOI: 10.1055/s-2006-957563
- (61) Wayne, P., *Reference Method for Broth Dilution Antifungal Susceptibility Testing of Yeasts*, Approved Standard. CLSI document M27-A2. **2002**.
- (62) *Methods for dilution antimicrobial susceptibility tests for bacteria that grow aerobically; approved standard*. 9th ed., Clinical and Laboratory Standards Institute, Wayne, PA, 2012.
- (63) Saraç, H.; Demirbaş, A.; Daştan, S. D.; Ataş, M.; Çevik, Ö.; Eryugur, N., Evaluation of nutrients and biological activities of kenger (*Gundellia tournefortii* L.) seeds cultivated in Sivas Province. *Turk. J. Agric. Food Sci. Technol.* **2019**, *7*, 52–58. DOI:10.24925/TURJAF.V7ISP2.52-58.3126
- (64) Erel, O., A new automated colorimetric method for measuring total oxidant status. *Clin. Biochem.* **2005**, *38*, 1103–1111. DOI:org/10.1016/j.clinbiochem.2005.08.008
- (65) Hlavac, F.; Rouer, E., Expression of the protein-tyrosine kinase p56lck by the pTRX vector yields a highly soluble protein recovered by mild sonication. *Protein Expr. Purif.* **1997**, *11*, 227–232. DOI: org/10.1006/prep.1997.0791
- (66) Laemmli, U. K., Cleavage of structural proteins during the assembly of the head of bacteriophage T4. *Nature.* **1970**, *227*, 680–685. DOI: 10.1038/227680a0
- (67) Blois, M. S., Antioxidant determinations by the use of a stable free radical. *Nature.* **1958**, *181*, 1199–1200. DOI:org/10.1038/1811199a0
- (68) Koparir, P.; Sarac, K.; Omar, R. A., Synthesis, molecular characterization, biological and computational studies of new molecule contain 1, 2, 4-triazole, and coumarin bearing 6, 8-dimethyl. *Biointerface Res. Appl. Chem.* **2022**, *12*, 809–823. DOI:org/10.33263/BRIAC121.809823